Supplementary Data

The stem cell-specific protein TRIM71 inhibits maturation and activity of the pro-differentiation miRNA let-7 via two independent molecular mechanisms

Lucia A. Torres-Fernández*, Sibylle Mitschka*, Thomas Ulas*, Stefan Weise, Kilian Dahm, Matthias Becker, Kristian Händler, Marc Beyer, Julia Windhausen, Joachim L. Schultze and Waldemar Kolanus

Submitted to *RNA* on 29.01.2021. Accepted on 29.04.2021.

Supplementary Figure 1

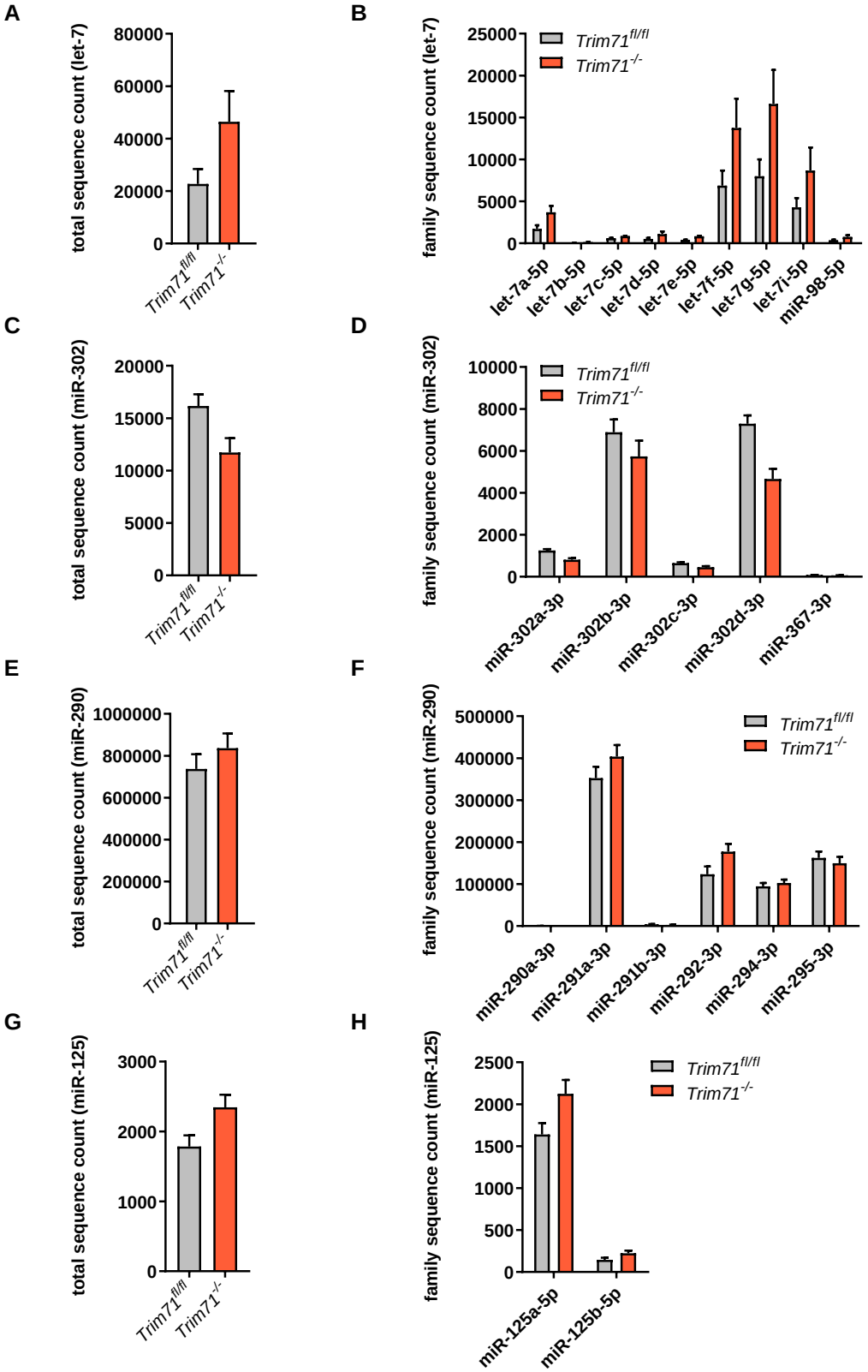

Supplementary Figure 1 (relative to Figure 1). Let-7 miRNAs are upregulated in TRIM71-deficient ESCs. Sequence counts (DESeq2 normalized counts) for the indicated miRNA families, obtained from our previously published dataset (GSE62509)[11] conducted in wild type (WT, *Trim71*$^{fl/fl}$) and *Trim71* knockout (KO, *Trim71*$^{-/-}$) ESCs. Integrated counts for all members together (left) or individual counts for each miRNA member of the indicated family (right) are shown. Error bars represent SD (n = 4-5).

Supplementary Figure 2

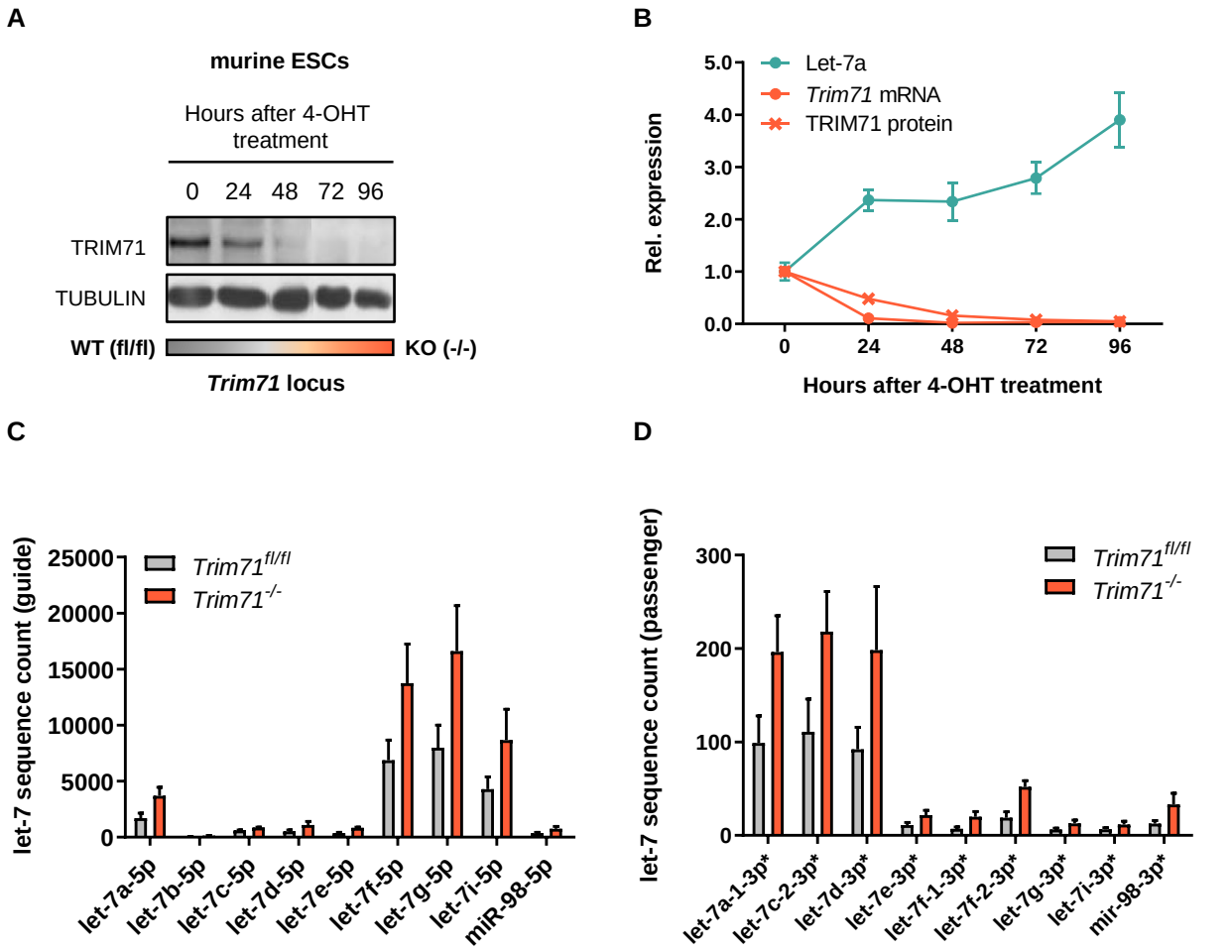

Supplementary Figure 2 (relative to Figure 1). Let-7 miRNAs are upregulated in TRIM71-deficient ESCs. A) Representative immunoblot showing endogenous TRIM71 levels in wild type (WT, *Trim71*$^{fl/fl}$) ESCs, and its downregulation over time upon 4-hydroxytamoxifen (4-OHT) treatment during *Trim71* knockout (KO, *Trim71*$^{-/-}$) ESCs generation. **B)** RT-qPCR showing the gradual upregulation of let-7 over time upon 4-OHT treatment during *Trim71* KO ESCs generation, concomitant to the gradual downregulation of TRIM71 protein (corresponding to A) and mRNA levels. RT-qPCR quantification of miRNAs and mRNAs was normalized to the levels of the housekeeping U6 snRNA and *Hprt* mRNA, respectively. **C)** Sequence counts (DESeq2 normalized counts) for mature let-7 guide (5p) and **D)** passenger (3p*) strands, obtained by the analysis of our previously published miRNASeq dataset (GSE62509)[11] conducted in wild type (WT, *Trim71*$^{fl/fl}$) and *Trim71* knockout (KO, *Trim71*$^{-/-}$) ESCs. Error bars represent SD (n = 4-5).

Supplementary Figure 3

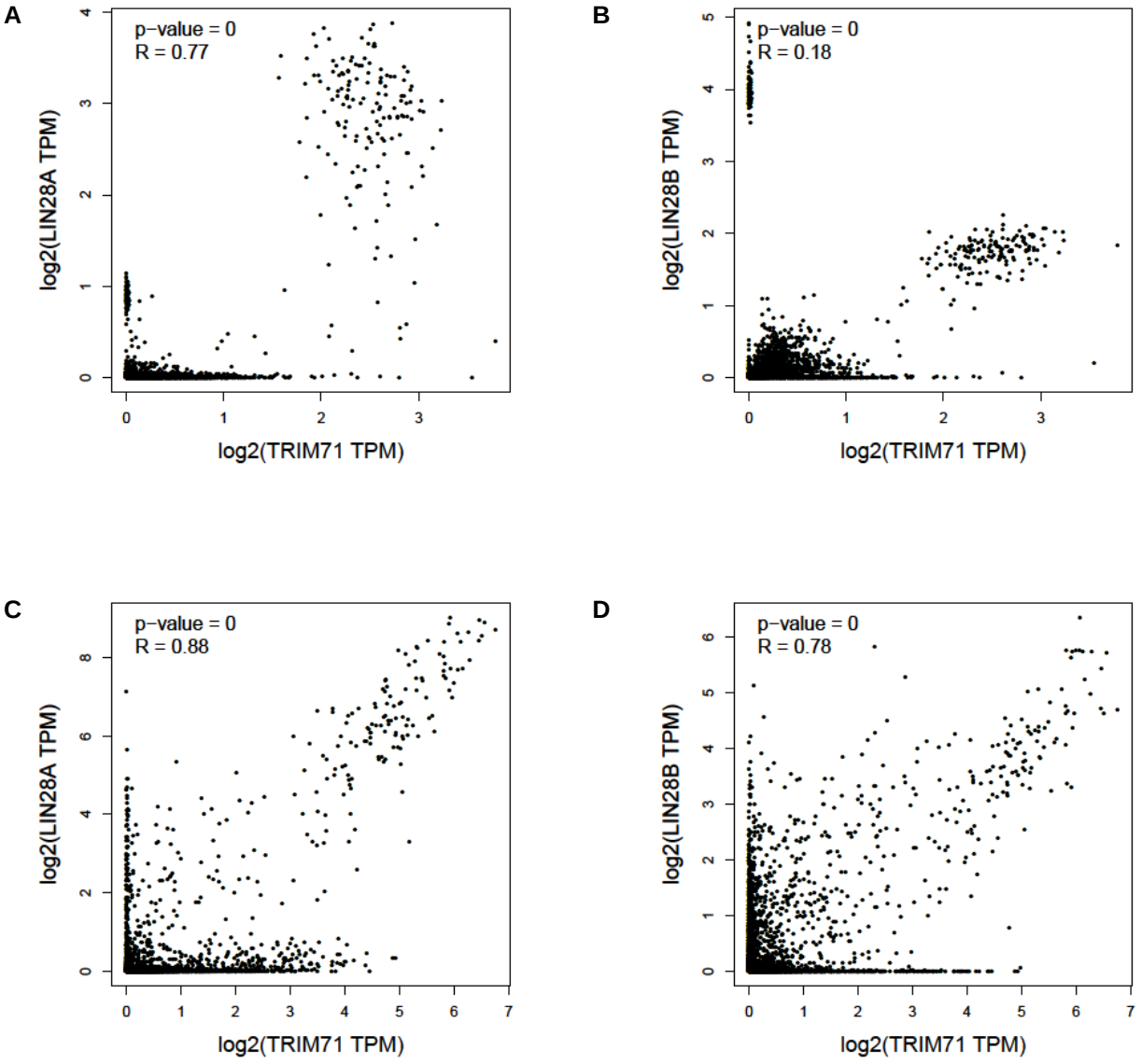

Supplementary Figure 3 (relative to Figure 2). The expression of *TRIM71* and *LIN28A/B* is positively correlated in human healthy and tumor samples. A) Correlation between the mRNA expression of *TRIM71* and *LIN28A* or **B)** *LIN28B* in healthy human tissues, obtained from GEPIA. All available healthy human tissues were included. **C)** Correlation between the mRNA expression of *TRIM71* and *LIN28A* or **D)** *LIN28B* in human tumor samples, obtained from GEPIA. All available human tumors were included. A significant positive correlation (***P-value<0.005, Pearson's coefficient) is observed for all cases.

Supplementary Figure 4

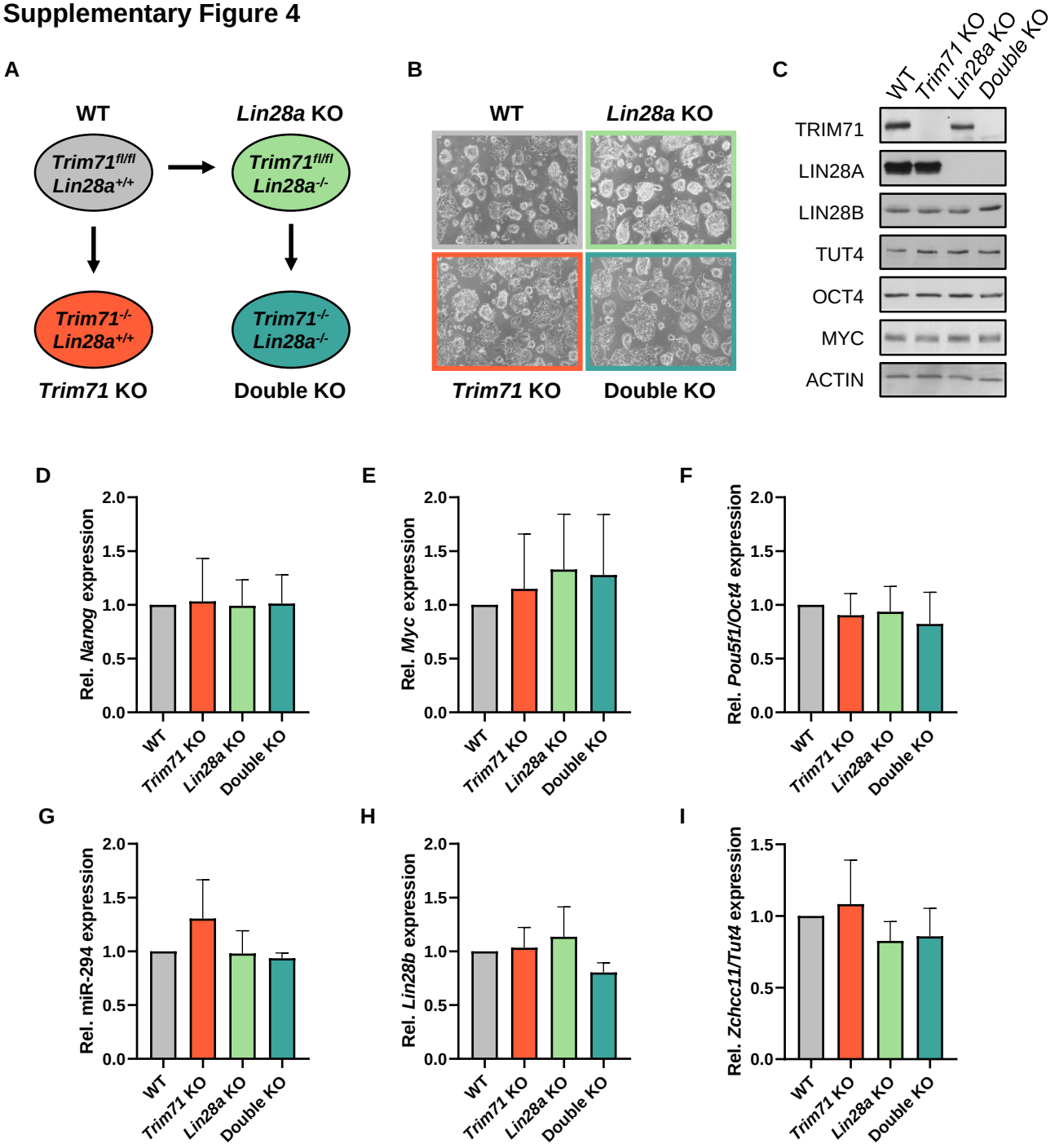

Supplementary Figure 4 (relative to Figure 3). Stemness is not compromised in *Trim71* KO, *Lin28a* KO or double KO ESCs. A) Schematic representation for the generation of the indicated ESC lines. *Lin28a* KO ESCs were generated from WT (*Trim71*$^{fl/fl}$) ESCs via TALENs. *Trim71* KO and *Trim71-Lin28a* double KO were generated by addition of 4-OHT to WT and *Lin28a* KO ESCs, respectively (see Methods for details). **B)** Bright field microscopic images of the different ESC lines, showing no major morphological changes between them. Images were taken at 5x magnification. **C)** Immunoblot showing the expression of the indicated proteins in the different ESC lines. **D)** RT-qPCR showing relative expression of *Nanog*, **E)** *Myc*, **F)** *Pou5f1/Oct4,* **G)** miR-294, **H)** *Lin28b* and **I)** *Zchcc11/Tut4* in the different ESC lines (n=3-7). RT-qPCR quantification of miRNAs and mRNAs was normalized to the levels of the housekeeping U6 snRNA and *Hprt* mRNA, respectively. Error bars represent SD. No significant differences were found between WT and any of the KO ESCs for all measured mRNAs/miRNA (unpaired Student's t-test).

Supplementary Figure 5

A

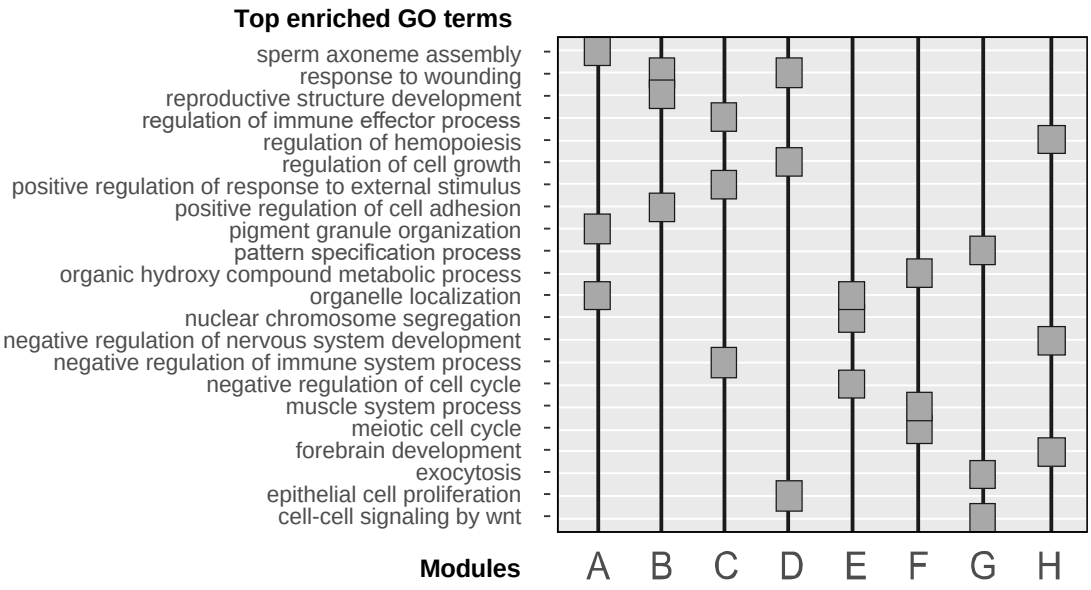

B

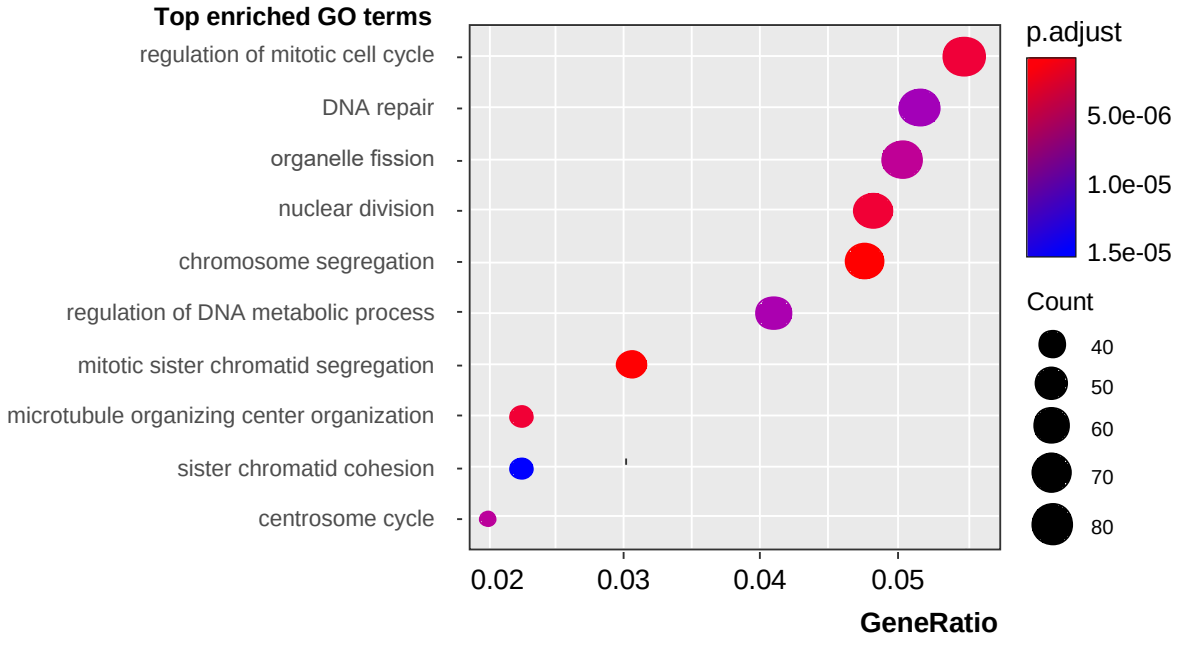

Supplementary Figure 5 (relative to Figure 3). Gene ontology (GO) term enrichment analysis. A) Top 3 enriched GO terms for each gene module found by co-expression network analysis of WT, *Trim71* KO, *Lin28a* KO and double KO ESC transcriptomes (depicted in main Fig. 3D). **B)** Top 10 enriched GO terms for let-7 targets found within modules B and E (depicted in main Fig. 3E) from co-expression network analysis of WT, *Trim71* KO, *Lin28a* KO and double KO ESC transcriptomes (depicted in main Fig. 3D). P.adjust = adjusted P-value.

Supplementary Figure 6

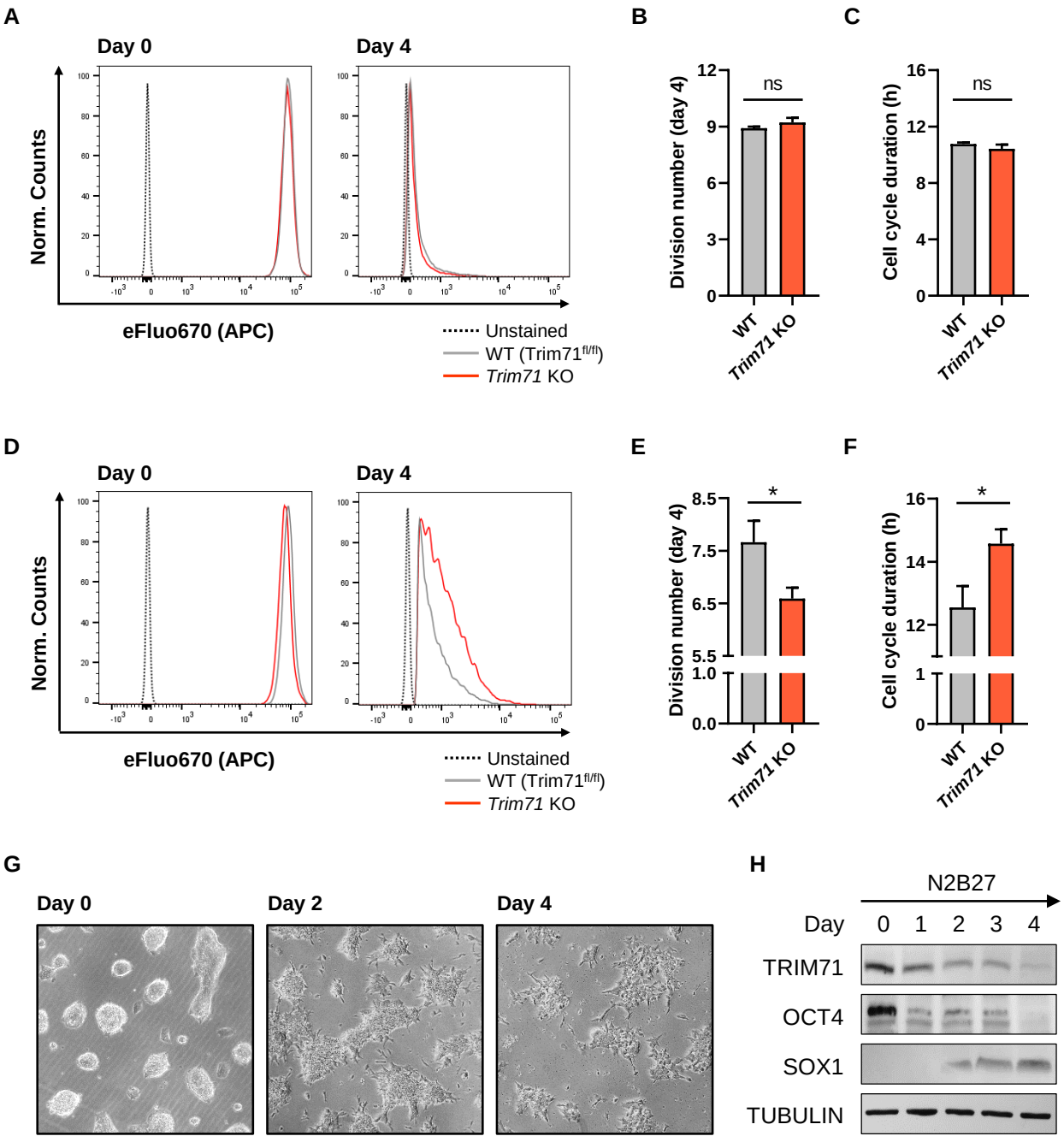

Supplementary Figure 6 (relative to Figure 3 and Suppl. Figure 5). TRIM71 controls proliferation in the course of neural differentiation. A) Representative flow cytometry eFluo670 (APC) histograms for the proliferation assays with wild type (WT, *Trim71*$^{fl/fl}$) and *Trim71* knockout (KO, *Trim71*$^{-/-}$) ESCs under steady state conditions. **B)** Number of cell divisions undergone at the end of the experiment (day 4) by WT and *Trim71* KO ESCs. The number of divisions was calculated assuming that the MFI of the proliferation dye eFluo670 (APC) decreases by half upon each cell division, as log2 [(MFI_{day0} – $MFI_{unstained}$)/(MFI_{day4} - $MFI_{unstained}$)]. (n = 3). **C)** Average duration of the cell cycle in hours (h) for WT and *Trim71* KO ESCs, calculated by dividing the total experimental time (4 days = 96 h) by the number of cell divisions (n = 3-6). **D)** Representative flow cytometry eFluo670 (APC) histograms for the proliferation assays with WT and *Trim71* KO ESCs in the course of N2B27-induced differentiation into neural progenitor cells (NPCs). Note a comparable eFluo670 (APC) fluorescence intensity for the different cell populations after staining (day 0) and the differences in fluorescence intensity at the end of the experiment (day 4). A slower loss of fluorescence intensity over time is apparent in *Trim71* KO histograms as compared to WT cells, and is indicative of a decreased proliferation (n = 3). **E)** Number of cell divisions undergone at the end of the N2B27-induced neural differentiation (day 4) by WT and *Trim71* KO cells, calculated as specified in B (n = 3). **F)** Average duration of the cell cycle in hours (h) for WT and *Trim71* KO cells, calculated by dividing the total experimental time (4 days = 96 h) by the number of cell divisions (n = 3). Error bars represent SD. *P-value < 0.05, ns = non-significant (unpaired student's t-test). **G)** Bright field microscopic images (10x magnification) of WT ESCs undergoing N2B27-induced neural differentiation at day 0, day 2 and day 4, showing expected differentiation-associated morphological changes. **H)** Immunoblot of WT ESCs undergoing N2B27-induced neural differentiation at days 0-4, showing expected changes in the expression of TRIM71, the pluripotency factor OCT4 and the NPC-specific marker SOX1.

Supplementary Figure 7

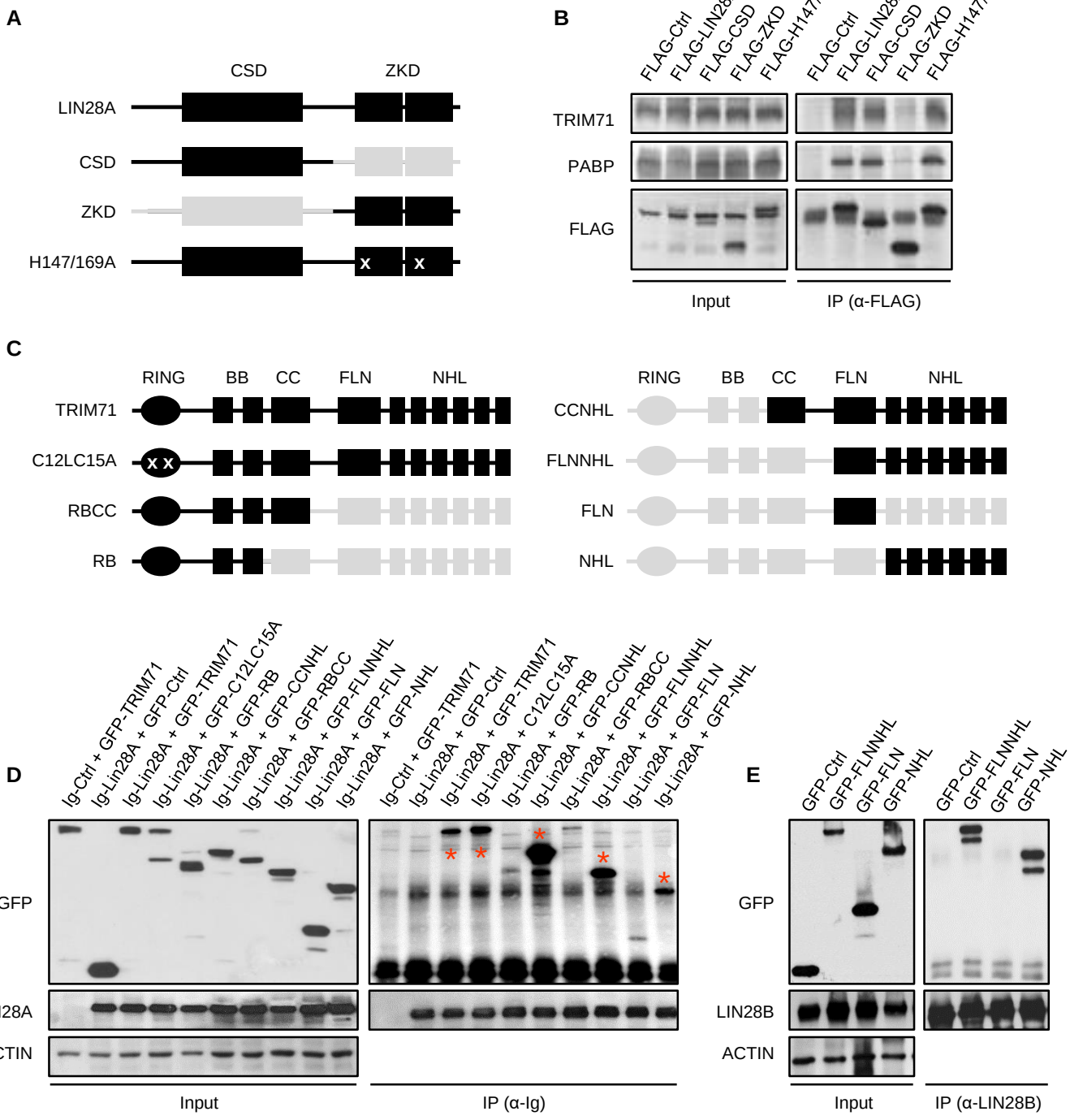

Supplementary Figure 7 (relative to Figure 4). TRIM71 interacts via its NHL domain with the CSD of LIN28 proteins. **A)** Schematic representation of LIN28A constructs used in B. For each construct, present domains are depicted in black, deleted domains are depicted in grey and mutations are marked with a white "x". **B)** Representative immunoblot showing the co-precipitation of endogenous TRIM71 with different Ig-tagged LIN28A constructs – depicted in A – overexpressed in wild type ESCs cells. PABP was used as control of a LIN28A binding partner. **C)** Schematic representation of TRIM71 constructs used in experiments depicted in D-E. For each construct, present domains are depicted in black, deleted domains are depicted in grey and mutations are marked with a white "x". **D)** Representative immunoblot showing the co-precipitation of different GFP-tagged TRIM71 constructs – depicted in C – with Ig-tagged LIN28A overexpressed in HEK293T cells. TRIM71 constructs co-precipitated with Ig-LIN28A to at least the same extent as the wild type full length TRIM71 protein are marked in the IP fraction with a red asterisk. **E)** Representative immunoblot showing the co-precipitation of different GFP-tagged TRIM71 constructs – depicted in C – with endogenous LIN28B in HEK293T cells.

Supplementary Figure 8

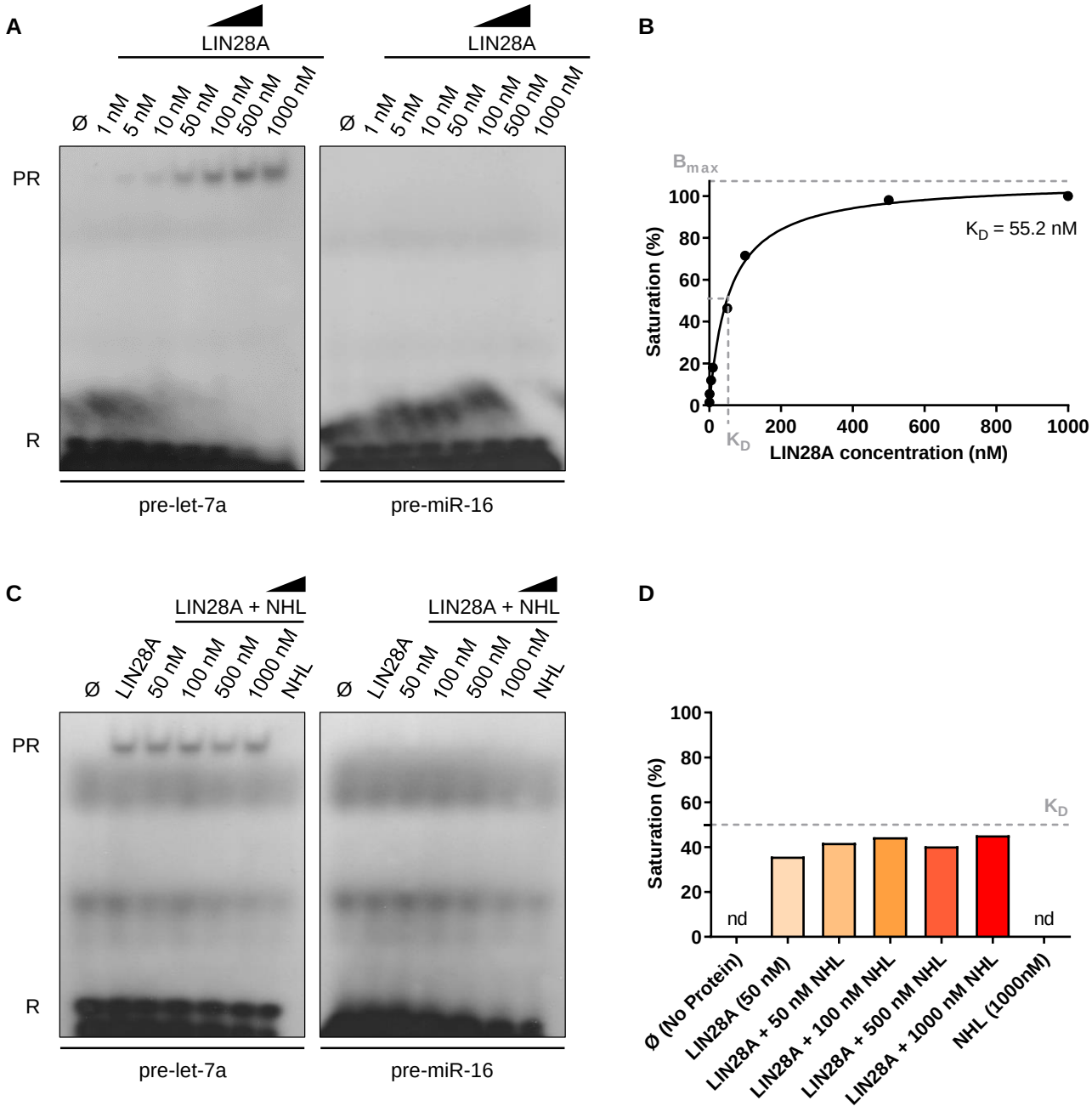

Supplementary Figure 8 (relative to Figure 5). The interaction between TRIM71 and LIN28A is facilitated by other cellular components. A) Electrophoretic mobility-shift assay (EMSA) performed with increasing concentrations of recombinant MYC-tagged LIN28A protein and a fixed amount of ^{32}P-labelled pre-let-7a or pre-miRNA-16. **B)** LIN28A binding curve derived from the Protein-RNA complexes (PR) band intensities from A, representing the binding between LIN28A and pre-let-7. The dissociation constant (K_D) was estimated from the graph equation $Y = (B_{max} * X)/(K_D + X)$. **C)** EMSA performed with 50 nM of MYC-tagged LIN28A and a fixed amount of ^{32}P-labelled pre-let-7a or pre-miR-16 in the presence of increasing concentrations of recombinant FLAG-tagged TRIM71 NHL protein. The capability of the NHL domain alone to bind pre-miRNAs was also tested (last lane) by using 1000 nM of NHL protein. **D)** Quantification of the LIN28A saturation levels reached in the absence and presence of increasing concentrations of NHL, calculated based on the PR band intensities of C. The dash line at 50% saturation levels (K_D threshold) represents the approximated maximal saturation that can be reached for the used LIN28A concentration (50 mM), according to experiments depicted in A-B. Ø = No Protein. PR = Protein-RNA complex. R = free ^{32}P-labelled pre-miRNA.

Supplementary Figure 9

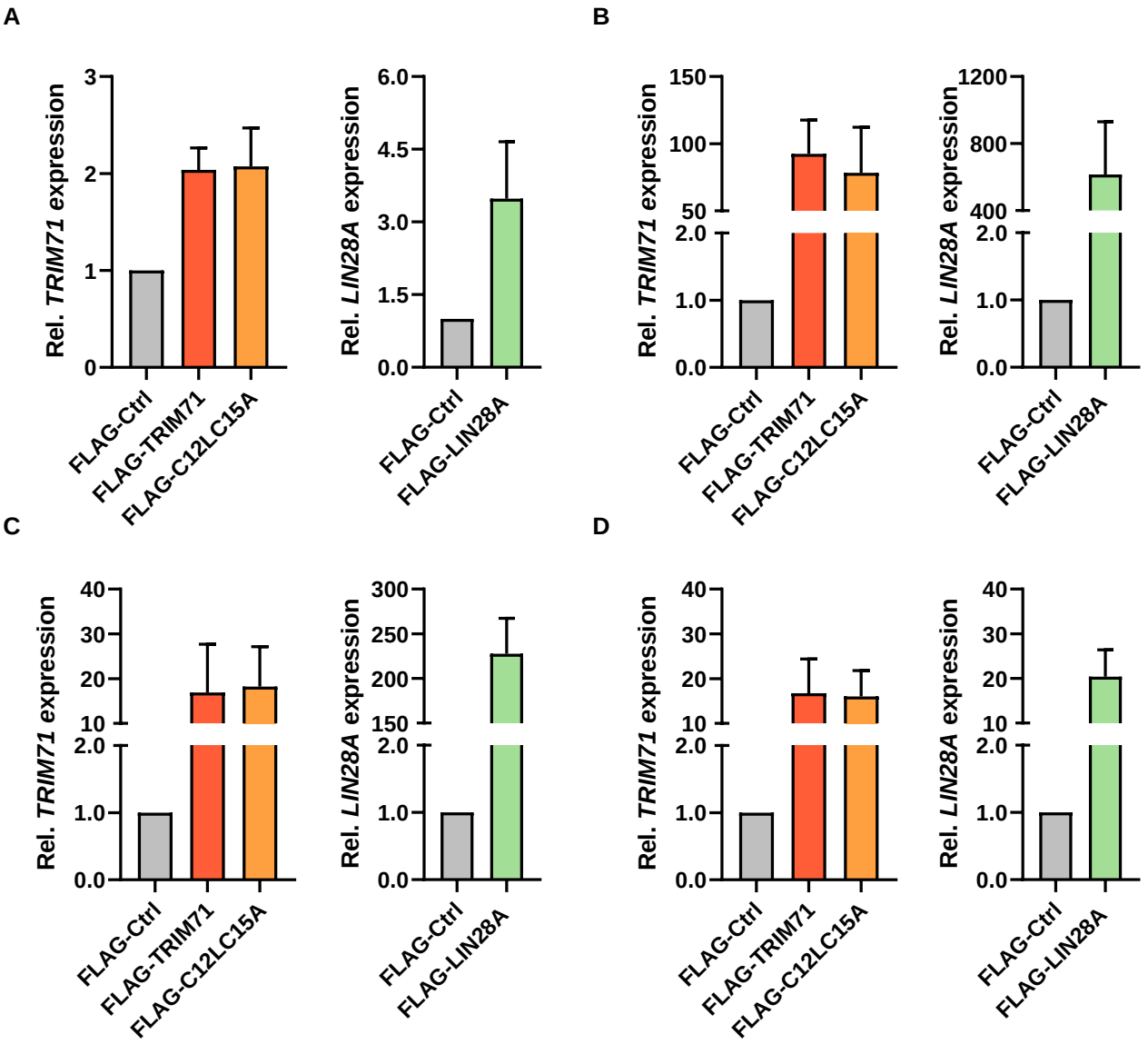

Supplementary Figure 9 (relative to Figure 6). RT-qPCR measurements after overexpression of FLAG-tagged wild type TRIM71, ubiquitination mutant C12LC15A and wild type LIN28A in several cell lines. A) *TRIM71* (left) and *LIN28A* (right) expression in ESCs, **B)** HEK293T cells, **C)** NIH3T3 and **D)** Jurkat E6.1 cells to control overexpression levels of the indicated FLAG-tagged constructs (n = 3). Note that, for each cell line, comparable levels of *TRIM71* are detected upon FLAG-TRIM71 and FLAG-C12LC15A overexpression, excluding that the differences observed for the regulation of let-7 derive from distinct transfection efficiencies.

Supplementary Figure 10

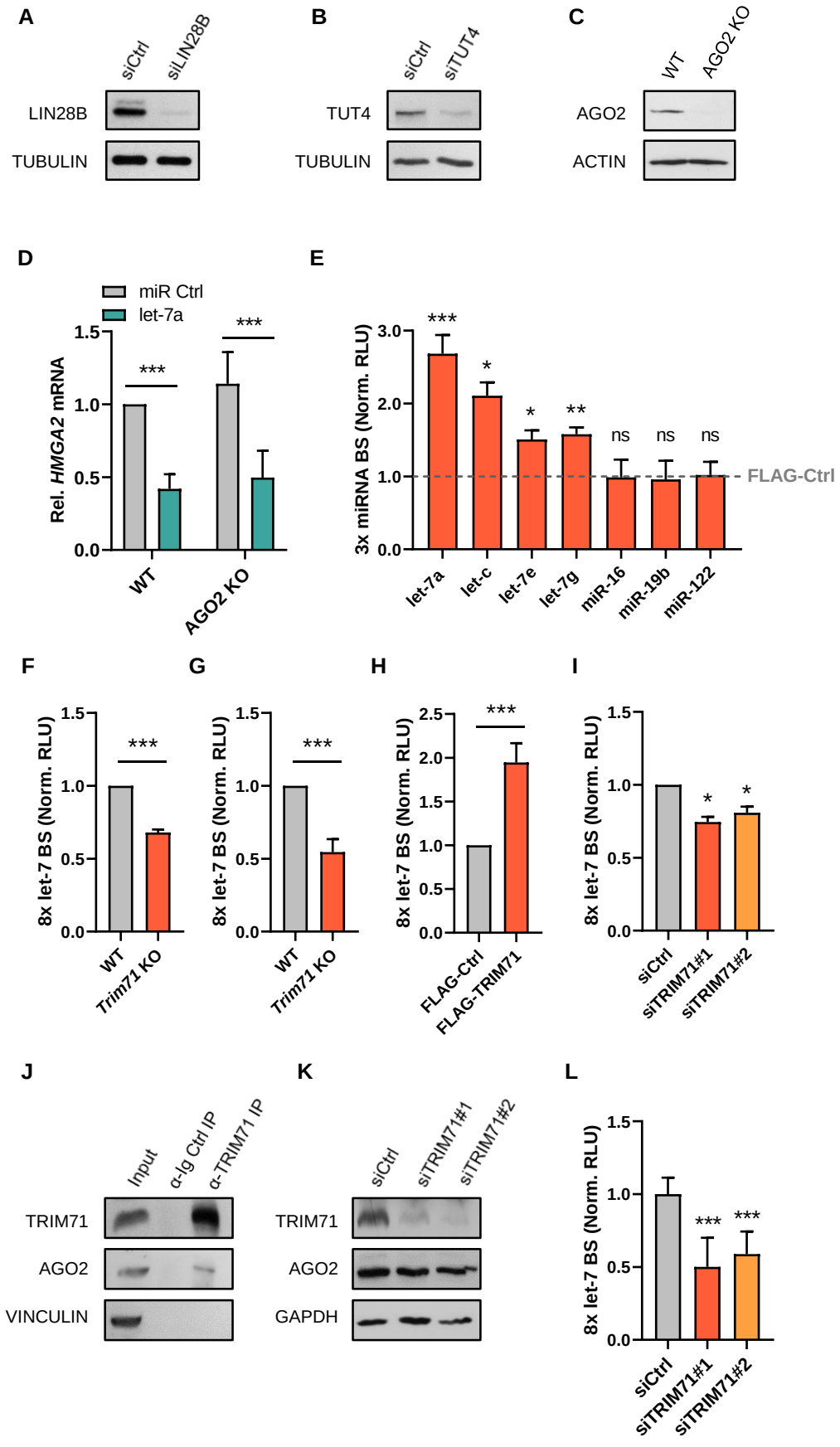

Supplementary Figure 10 (relative to Figures 7-9). The AGO2-dependent TRIM71-mediated miRNA activity regulation mechanism. A) Representative immunoblots showing levels of LIN28B protein after LIN28B knockdown (siLIN28B), **B)** TUT4 protein after TUT4 knockdown (siTUT4) in HEK293T cells, and **C)** AGO2 protein in WT and AGO2 KO HEK293T cells. **D)** RT-qPCR showing the expression of the *bona fide* let-7 target *HMGA2* mRNA after overexpression of a control miRNA duplex (miR Ctrl) or mature let-7 miRNA duplex in WT and AGO2 KO HEK293T cells (n=4). The housekeeping gene *HPRT1* was used for normalization. **E)** miRNA reporter assays after FLAG-Ctrl (represented by the dashed line) and FLAG-TRIM71 overexpression in HEK293T cells. Overexpression of each respective miRNA duplex resulted in a significant repression of each reporter, respectively (data not shown), proving the functionality of the newly-generated reporter constructs, which contained 3x miRNA binding sites (BS) in tandem in the 3'UTR downstream of a Renilla luciferase coding sequence. Norm. RLU = normalized relative light units. **F)** Let-7 reporter assay in WT and *Trim71* KO murine ESCs (n = 3). **G)** Let-7 reporter assay in WT and *Trim71* KO murine neuroectodermal NE4C cells (n = 5). **H)** Let-7 reporter assay in human embryonic carcinoma NCCIT cells upon TRIM71 overexpression (n = 4) and **I)** TRIM71 knockdown with two different siRNAs (siTRIM71 #1 and #2) (n = 4). **J)** Immunoblot showing the co-precipitation of endogenous AGO2 with endogenous TRIM71 in human hepatocellular carcinoma HepG2 cells. **K)** Immunoblot showing AGO2 protein levels upon TRIM71 knockdown in HepG2 cells with two different siRNAs (siTRIM71 #1 and #2). **L)** Let-7 reporter assay in HepG2 cells upon TRIM71 knockdown with two different siRNAs (siTRIM71 #1 and #2) (n = 4). Norm. RLU = normalized relative light units. Error bars represent SD. ***P-value < 0.005, **P-value < 0.01, *P-value < 0.05, ns = non-significant (unpaired student's t-test between FLAG-Ctrl/siCtrl and each other condition, unless indicated by a line joining the two compared conditions).

Supplementary Materials Tables

Materials Table 1

miRNA mimics	Reference number (MirVana)
miR Ctrl	4464059
Let-7a-5p	MC10050
Let-7g-5p	MC11758
miR-16-5p	MC10339
miR-19b-2-3p	MC10629
pre-let-7a	PM10050
pre-mir-16	PM10339

Materials Table 2

siRNAs	Sequence (5'-3')
siCtrl	AAACATGCAGAAAATGCTG
siLIN28B	GGAAGGAUUUAGAAGCCUAAA
siTUT4/ZCCHC11	GGAGCACAUAAACAUAUAATT
siTRIM71#1	CCGTGTGCGACCAGAAAGTA
siTRIM71#2	CCAGATCTGCTTGCTGTGCAA

Materials Table 3

RT-qPCR Taqman probes	Reference number (Applied Biosystems)
let-7a-3p*	#002478
let-7a-5p	#000377
let-7g-3p*	#002492
let-7g-5p	#002282
miR-16-3p	#000391
miR-125a-3p	#002199
miR-294-3p	#001056
miR-302a-3p	#000529
u6 snRNA	#001973
pri-let-7a	Hs03302539_pri
pre-let7a	Hs04231409_s1
Lin28a	Mm00524077_m1
Lin28b	Mm01190673_m1
Myc	Mm00487804_m1
Nanog	Mm02384862_g1
Pou5f1/Oct4	Mm03053917_g1
Trim71	Mm01341471_m1
Zchcc11/Tut4	Mm00615428_m1
TRIM71	Hs01394933_m1
LIN28A	Hs04189307_g1
LIN28B	Hs01013729_m1
HMGA2	Hs00171569_m1

Materials Table 4

Antibodies (predicted size)	Company (reference number)
Goat anti-IgG (39.7 kDa)	Jackson Immuno Research (109-005-098)
Mouse anti-FLAG M2 (1 kDa)	Sigma-Aldrich (F1804)
Mouse anti-GAPDH (36 kDa)	Acris (ACP001P)
Mouse anti-GFP (32.7 kDa)	Santa Cruz Biotechnology (sc-9996)
Mouse anti-TUBULIN (50 kDa)	Sigma-Aldrich (T9026)
Mouse anti-VINCULIN (123.8 kDa)	Sigma-Aldrich (V9131)
Rabbit anti-ACTIN (41.7 kDa)	Sigma-Aldrich (A2066)
Rabbit anti-LIN28A (23 kDa)	Cell Signaling Technology (8641)
Rabbit anti-LIN28B (30 kDa)	Cell Signaling Technology (4196)
Rabbit anti-PABP (70.7 KDa)	Santa Cruz Biotechnology (sc-28834)
Rabbit anti-TRIM71 (93.4 kDa)	Sigma-Aldrich (HPA038142)
Rabbit anti-TUT4/ZCCHC11 (185 kDa)	Proteintech Group (18980-1-AP)
Rat anti-AGO2 (93.6 kDa)	Sigma-Aldrich (SAB4200085)
Rabbit anti-OCT4 (38 kDa)	Abcam (ab18976)
Mouse anti-MYC (62 kDa)	Santa Cruz Biotechnology (sc-40)
Rabbit anti-SOX1 (40 kDa)	Cell Signaling Technology (4194)